Elasticity of Nematic Networks and Nematic Effects in Conventional Rubbers

P. Bladon* and M. Warner

Theory of Condensed Matter, Cavendish Laboratory, Madingley Road, Cambridge CB3 OHE, U.K.

Received July 16, 1992; Revised Manuscript Received November 9, 1992

ABSTRACT: Nematic rubbers are composed of cross-linked polymer chains with stiff rods either incorporated into their backbones or pendant as side chains. When nematic effects are strong, such rubbers exhibit discontinuous stress–strain relationships and spontaneous shape changes. We model such a rubber using Gaussian elasticity theory, including the nematic interaction via a mean field. Results are presented for the cases of uniaxial compression and biaxial extension, and unusual phase transitions are obtained. When nematic effects are very small (i.e., $T \gg T_c$, where T_c is the nematic–isotropic phase transition temperature of the rubber) we postulate that the model is a good approximation to a conventional, nonnematic elastomer and fit our model to data from an isoprene rubber.

1. Introduction

Nematic networks are formed by cross-linking nematic polymers, polymers with nematic units incorporated into the main chain or hung as pendants from the main chain. In this paper we shall describe only the case of main-chain polymer liquid crystals (PLCs). However, there exist many types of side-chain PLCs of the same symmetry and our analysis will apply qualitatively to them as well. The cross-linking of PLCs into a network allows the nematic orientational ordering of the polymer chains to couple to the mechanical properties of the network as first envisaged by de Gennes,[1,2] who predicted unusual consequences such as mechanically induced phase transitions, discontinuous stress–strain relationships with associated mechanical critical points, and solids exhibiting spontaneous shape changes upon cooling, effects which have now been experimentally confirmed.[3-8] When a rubber is stressed, the shape of the polymeric chain between cross-links is distorted away from the equilibrium shape distribution. In a PLC melt, upon cooling through the phase transition point, the shape of the chains spontaneously changes as the nematic orients itself. These two effects are used in the formulation of a theory of nematic rubbers. The deviations of chain shape away from the equilibrium melt values cause the nematic free energy to rise. This can be offset by the change in the elastic free energy caused by altering the chain shape. This cross-coupling between the nematic and elastic free energies leads to the unusual properties of network PLCs. Cross-linking PLCs at different temperatures (above and below their T_c's, where T_c is the isotropic–nematic phase transition temperature), affects the properties of nematic rubbers. This was again predicted by de Gennes, quantified by Warner et al.[9] and later seen experimentally.[3,5,7]

In this paper we discuss the effects on a model nematic rubber of compression and biaxial extension. The rubber is modeled as simply as possible using a mean field nematic interaction that is uniaxial; i.e., the effective geometry of the mesogenic components is cylindrical. Under uniaxial compression a rubber above its isotropic–nematic phase transition first forms a paranematic uniaxial oblate phase. Increasing the stress beyond a certain point causes a phase transition to a biaxial state, where the nematic effect tries to align the rubber uniaxially in a direction perpendicular to the stress. A tricritical point is found where the mechanically induced phase transition changes from first to second order. Under biaxial extension a biaxial paranematic state exists, and a full range of behavior of isotropic → paranematic biaxial → biaxial nematic states is found.

We believe that deviations away from the classical rubber elasticity of Gaussian chains in real rubbers can be accounted for by residual nematic interactions, as do other authors.[10-12] A previous version of this theory that could not allow for biaxial order showed deviations away from classical elasticity which were of the right type.[13] A conventional elastomer with small nematic interactions can be represented by a nematic rubber with $T \gg T_c$, where in the conventional rubber the nematic-phase transition cannot be reached because it lies below the glass transition temperature. It is not sufficient for a theory to explain only uniaxial stress–strain behavior; the whole range of possible elastic behavior must be accounted for. We therefore fit our theory to the conventional Mooney plot for uniaxial stress–strain and use the best-fit parameters obtained to compare to biaxial data, as suggested by Gottlieb and Gaylord.[14] Various authors have extended the theory of Gaussian chain rubber to include the aligning effect of excluded-volume interactions between extended chains.[15-18] Incorporation of these effects gives deviations away from the Gaussian theory which are qualitatively of the right type, but not necessarily of the right size to explain the experimentally observed deviations. References 16 and 18 have similarities to the present work in that they both lead to anisotropic Guassian chains.

In section 2, we review the theory of nematic wormlike polymers and how the nematic contribution to the free energy and chain shape can be calculated. In section 3, we discuss the theory of Gaussian elasticity and couple the two halves of the theory together. In section 4.1, we compare our theory of nematic rubber with small nematic interactions to data for conventional rubbers. In section 4.2, we present numerical results for uniaxial compression and biaxial extension of a nematic rubber, and in section 5, we conclude.

2. A Model for PLCs

2.1. Order Parameter. The nematic polymer is modeled using a worm chain theory, where the polymer is represented by a continuous curve. The polymer is locally inextensible and has its own intrinsic stiffness and nematicity. The nematic effects are included via a mean field theory whereby each infinitesimal element of the chain contributes to an effective self-consistent field which

0024-9297/93/2226-1078$04.00/0

replaces the individual pair interactions between elements. First, suitable order parameters must be chosen to characterize the system, as must a suitable pseudopotential in terms of the self-consistent mean field order parameters. The nematic phase of a liquid is characterized by the long-range orientational order of the constituent molecules. This results in the response functions of the bulk material, i.e., the diamagnetic susceptibility, dielectric permittivity, being anisotropic. The order parameter matrix, a traceless symmetric second-rank tensor, describes this anisoptropy. As the tensor is symmetric it is always possible to find a frame of reference in which it is diagonal. A conventional parameterization (see ref 19) is

$$\mathbf{Q}_{\alpha\beta} = \begin{pmatrix} \left(-\frac{1}{2}Q + \frac{1}{2}X\right) & 0 & 0 \\ 0 & \left(-\frac{1}{2}Q - \frac{1}{2}X\right) & 0 \\ 0 & 0 & Q \end{pmatrix} \quad (1)$$

Q and X are themselves known as order parameters and are just numbers that characterize the physical system. This parameterization allows for the existence of truely biaxial and three, equivalent, uniaxial phases. The uniaxial phases are $Q_1 \neq 0$, $X_1 = 0$; $Q_2 \neq 0$, $X_2 = \pm 3Q_2$, which correspond to uniaxial alignment along the z, y, and x axes, respectively. When the previous relations are not obeyed, the phase is biaxial. When z is the unique axis, X measures the biaxiality of the phase. If, however, the same system is viewed from the x or y axis, X no longer directly measures the biaxiality. The biaxiality can be extracted by determining the largest element of the order parameter matrix, whereupon the biaxiality is the difference between the other two elements. The other choices of characterizing uniaxial phases are mentioned because the phase transition from an oblate to a transversely squashed prolate phase changes the unique axis. This transition occurs as we apply an external field (stress) to a nematic polymer.

The orientational pseudopotential for a mean field theory of uniaxial (cylindrical) objects is as follows:[20]

$$U(u,\phi) = aQP_2(u) + \frac{aX}{2}(1-u^2)\cos(2\phi) \quad (2)$$

with

$$Q = \overline{P_2(u)} \quad (3)$$

$$X = \overline{\frac{3}{2}(1-u^2)\cos(2\phi)} \equiv \overline{\frac{1}{2}P_2^2(u)\cos(2\phi)} \quad (4)$$

$P_2(u)$ and $P_2^2(u)$ are Legendre polynomials and $u = \cos(\theta)$, θ and ϕ being respectively the polar and azimuthal angles that each nematogen makes with the director, the z axis. a is the interaction energy constant. Q and X in the macroscopic order parameter (1) are therefore the orientational averages of the nematogens in the mean field pseudopotential. Q takes values between −0.5 and 1.5 and X between −1.5 and 1.5. The biaxial order parameter X is indirectly dependent on the uniaxial order parameter Q since it depends on $(1-u^2) \equiv \sin^2(\theta)$. If the molecules are well ordered, $u \to 1$; $\theta \to 0$ or π and hence $Q \to 1$ and then $X \to 0$. Thus making a biaxial phase more ordered (say, by lowering the temperature) will reduce the biaxiality.

We emphasize that our chains are the simplest imaginable with no intrinsic biaxiality in their interactions; i.e., the coupling a in (2) is common to both the QP_2 and XP_2^2 terms. More elaborate effects could be put in by adopting distinct coupling constants in the two parts of eq 2.

2.2. Wormlike Chain Model of a Nematic Polymer. A worm chain in a nematic field has been reduced to a spheroidal wave equation by a number of authors.[21-24] The chain is represented as a continuous curve where a point on the chain is given by $\mathbf{r}(s)$, s being the chemical length along the chain from one end. Denoting $\partial/\partial s$ by $'$ and $\mathbf{r}'(s)$ by $\mathbf{u}(s)$—the tangent vector of the curve at s— the bending energy of the chain is given in terms of the total curvature of the chain and an elastic constant ϵ. The bending energy is then $\frac{1}{2}\epsilon\int_0^L ds|\mathbf{u}'(s)|^2$, where L is the total chain length. Each infinitesimal length of the chain feels and contributes to the nematic potential. The nematic energy of a chain in the nematic mean field is therefore $-aQ\int_0^L ds P_2(u_z(s)) - \frac{1}{2}aX\int_0^L ds(1-u_z(s)^2)\cos 2\phi(s)$, where a is now an energy per unit length and $u_z(s) = \cos\theta(s)$ is the component of the tangent vector in the z direction. The partition function is written as

$$Z = \int \delta\mathbf{u}(s) \exp\left(-\frac{1}{2}\beta\epsilon\int_0^L ds\,|\mathbf{u}'(s)|^2 + \beta aQ \times \int_0^L ds\, P_2(u_z(s)) + \frac{\beta aX}{2}\int_0^L ds\,(1-u_z(s)^2)\cos 2\phi(s)\right) \quad (5)$$

where $\int\delta\mathbf{u}(s)$ represents a sum over all configurations of the chain. The differential equation corresponding to the partition function is

$$\left(\frac{\partial}{\partial s} - \frac{1}{l_0}\nabla^2 - \beta aQP_2(u_z) - \frac{\beta aX}{2}(1-u_z^2)\cos 2\phi\right) \times \Phi(\theta,\phi,s) = 0 \quad (6)$$

which represents the diffusion of the tangent vector $\mathbf{u}$ on the surface of the unit sphere with a diffusion constant $1/l_0 = (2\beta\epsilon)^{-1}$. l_0 is the effective step length of the chain, characterizing the worm chain in the absence of nematic fields.[25] Multiplying by l_0 and setting $\Phi = Sp_{n,m} \times \exp(-\lambda_{n,m}s/l_0)$, the wave equation becomes

$$(\lambda_{n,m} + \nabla^2 + \Delta_Q^2 P_2(u_z) + \Delta_X^2(1-u_z^2)\cos 2\phi)Sp_{n,m} = 0 \quad (7)$$

where the coupling constants $\Delta_Q^2 = \beta aQl_0$, $\Delta_X^2 = \beta aXl_0/2$ have been introduced. The Greens function for this wave equation is

$$G(\mathbf{u},\mathbf{u}_0;L,0) = \sum_{n,m} Sp_{n,m}(\mathbf{u})\, Sp_{n,m}(\mathbf{u}_0) \exp(-\lambda_{n,m}L/l_0) \quad (8)$$

Note that eq 7 is not the standard form of the zero-order spheroidal wave equation,[26] as the potential is of the form $\Delta_Q^2 P_2(u_z) + \Delta_X^2(1-u_z^2)\cos 2\phi$ rather than the standard $-u_z^2$-like term. The relationship between coupling constant and eigenvalues used by Warner et al. in previous work is $\Lambda_0 = \lambda_{0,0} - {}^2/_3\Delta^2$, where $\Delta^2 = -{}^2/_3\Delta_Q^2$. In this work normalize the $Sp_{n,m}$ wave functions to one instead of the normal value. These $Sp_{n,m}$ wave functions are the spheroid equivalent of the spheroidal functions $Y_l^m(\theta,\phi)$.

The propagator G can be used to evaluate the partition function and the conformations of the chain.[22]

$$Z = \int \mathbf{u}\,\mathbf{u}_0\, G(\mathbf{u},\mathbf{u}_0;L,0) \quad (9)$$

If the value of L is large, then the partition function, Z, becomes dominated by the first term and the term $-k_BT$ log Z in the free energy can be replaced by the lowest eigenvalue of the diffusion equation. This "long-chain" limit is analogous to ground-state dominance in a quantum

mechanical system at long times. The nematic free energy per chain can therefore be written as

$$\frac{F_{\text{nematic}}}{k_BT} = \lambda_{0,0}\frac{L}{l_0} + \frac{1}{2}\beta a Q^2 L + \frac{1}{6}\beta a X^2 L \tag{10}$$

where $\beta = 1/k_BT$. The extra two terms in the free energy arise from the mean field replacement of pair interactions by temperature single particle potentials.[27] It is more convenient computationally to work in terms of the coupling constants Δ_Q^2 and Δ_X^2. Then (10) becomes

$$\frac{F_{\text{nematic}}}{k_BT} = \frac{L}{l_0}\left(\lambda_{0,0} + (\Delta_Q^2)^2\frac{\tilde{T}^2}{4} + (\Delta_X^2)^2\frac{\tilde{T}^2}{3}\right) \tag{11}$$

where the reduced temperature $\tilde{T} = k_BT/(a\epsilon)^{1/2}$ has been introduced. The phase transition temperature for the melt is $\tilde{T} = \tilde{T}_c = 0.387\,75$.[24,27]

Using the long-chain limit, the radii of gyration of the chain are

$$\langle R_z^2\rangle = Ll_0\sum_{n,m}\frac{2}{\lambda_{0,0}^{n,m}}\left(\int \mathrm{d}\mathbf{u}\, Sp_{0,0}(\mathbf{u})\cos\theta Sp_{n,m}(\mathbf{u})\right)^2$$

$$\langle R_x^2\rangle = Ll_0\sum_{n,m}\frac{2}{\lambda_{0,0}^{n,m}}\left(\int \mathrm{d}\mathbf{u}\, Sp_{0,0}(\mathbf{u})\sin\theta\cos\phi Sp_{n,m}(\mathbf{u})\right)^2 \tag{12}$$

$$\langle R_y^2\rangle = Ll_0\sum_{n,m}\frac{2}{\lambda_{0,0}^{n,m}}\left(\int \mathrm{d}\mathbf{u}\, Sp_{0,0}(\mathbf{u})\sin\theta\sin\phi Sp_{n,m}(\mathbf{u})\right)^2$$

where the shorthand $\lambda_{0,0}^{n,m} = \lambda_{n,m} - \lambda_{0,0}$ has been used. The coefficients of $L/3$ in each case are the effective step lengths l_x, l_y, and l_z, respectively, of an anisotropic random walk. The propagator can be expressed using perturbation theory or numerically using a matrix diagonalization in the basis of the spherical harmonics.

3. Elastic Free Energy

As a polymer network is deformed, the conformations of the chains making up that network also change. If the shape change in a nematic network constrains the polymer to be away from its natural nematic shape, the nematic free energy has to rise. The classical theory of rubber elasticity is based on the assumption that the chain between cross-links is Gaussian. The probability of a chain having an end to end vector $\mathbf{R}$ is

$$P(\mathbf{R}) = \frac{1}{(2\pi l_0 L)^{3/2}}\left(\frac{l_0^3}{l_x l_y l_z}\right)^{1/2}\times \exp\left[-\left(\frac{3R_x^2}{2l_xL} + \frac{3R_y^2}{2l_yL} + \frac{3R_z^2}{2l_zL}\right)\right] \tag{13}$$

where R_x, R_y, and R_z are components of $\mathbf{R}$ in the coordinate system with z as the director. It is assumed that in the nematic network the chain is long enough, even when nematic and distorted, to remain a Gaussian, albeit anisotropic. The mean square end to end distances in this Gaussian approximation are

$$\langle R_i^2\rangle = \frac{1}{3}l_iL \tag{14}$$

and the effective step lengths l_x, l_y, and l_z determine the shape of the chain; see eq 14 for their origin. The cross-coupling between the nematic and elastic free energies occurs because the coefficients l_x, l_y, and l_z are functions of the order in the system; i.e., $l_x = l_x(Q,X)$, that is, chain shape depends on nematic order. After cross-linking, the assumption is made that a chain in the network deforms affinely with the bulk deformation λ because of the constraints of the cross-links. Thus, the end to end vector of a chain deforms to

$$\mathbf{R} = \lambda\cdot\mathbf{R}_0 \tag{15}$$

where λ is a symmetrical second-rank tensor. For a general distortion there are three principal extension ratios, λ_x, λ_y, and λ_z, which are the eigenvalues of λ. Because rubber is incompressible they must satisfy $\lambda_x\lambda_y\lambda_z = 1$. The additional elastic free energy of a strand of the network with deformed span $\mathbf{R}$ is

$$F_{\text{elastic}} = -k_BT\,\langle \log P(\mathbf{R})\rangle_{P_0} \tag{16}$$

where P_0 is the probability at cross-linking. If cross-linking is in the isotropic state, then P_0 is an isotropic Gaussian. Averaging one obtains

$$\frac{F_{\text{elastic}}}{k_BT} = \frac{1}{2}\left(\alpha_x\lambda_x^2 + \frac{\alpha_y}{\lambda_x^2\lambda_z^2} + \alpha_z\lambda_z^2\right) - \frac{1}{2}\log(\alpha_x\alpha_y\alpha_z) \tag{17}$$

α_x, α_y, and α_z are l_0/l_x, l_0/l_y, and l_0/l_z, respectively. In this paper we only concern ourselves with results for cross-linking in the isotropic state. Reference 9 gives the microscopic picture of how cross-linking in the nematic state elevates the phase transition in the network.

Combining (17) and (11), the total free energy per unit volume in units of k_BT is

$$F(Q,X,\lambda_x,\lambda_z)_{\text{total}} = N_s[F(Q,X)_{\text{nematic}} + F(Q,X,\lambda_x,\lambda_z)_{\text{elastic}}] \tag{18}$$

where N_s is the number density of strands. The free energy has to be minimized with respect to the order parameters Q and X, either by solving directly $\partial F/\partial Q|_{X,\lambda_x,\lambda_z} = \partial F/\partial X|_{X,\lambda_x,\lambda_z} = 0$ or by a direct minimization of the free energy. The equilibrium values of Q and X will be denoted by $\bar{Q}$ and $\bar{X}$, respectively.

There are several ways of calculating the stress–strain response of the system. One can work by fixing the extension ratios and then calculating the stresses (a Helmholtz ensemble) or by fixing the stresses and calculating the extension ratios (a Gibbsian ensemble).

In the Helmholtz case, stresses are calculated by evaluating $\sigma_i^*/\lambda_i = \partial E/\partial\lambda_i|_{Q,X,\lambda_{j\neq i}}$, where σ_i^* is the stress reduced by k_BT, i.e., σ_i/k_BT. Therefore, for a general deformation one obtains at equilibrium

$$\frac{\sigma_z}{k_BT} = \sigma_z^* = N_s\left(\alpha_z(\bar{Q},\bar{X})\lambda_z^2 - \frac{\alpha_y(\bar{Q},\bar{X})}{\lambda_x^2\lambda_z^2}\right)$$

$$\frac{\sigma_x}{k_BT} = \sigma_x^* = N_s\left(\alpha_x(\bar{Q},\bar{X})\lambda_x^2 - \frac{\alpha_y(\bar{Q},\bar{X})}{\lambda_x^2\lambda_z^2}\right) \tag{19}$$

In the Gibbs ensemble it is necessary to add work terms to the free energy like $-\sigma\log\lambda$. Therefore

$$G = F_{\text{total}} - \sigma_x^*\log\lambda_x - \sigma_z^*\log\lambda_z \tag{20}$$

For a general deformation the λ's have to be chosen to minimize G as well as the Q's and X's. The equations $\partial G/\partial\lambda_z|_{Q,X,\lambda_x} = \partial G/\partial\lambda_x|_{Q,X,\lambda_z} = 0$ can be solved analytically to find $\lambda(\sigma_x,\sigma_z,Q,X)$. The analytic form obtained for the λ's can then be substituted into (20) before minimizing for the Q's and X's.

When phase transitions are investigated, it is more natural to use the Gibbs ensemble as discontinuities in

the strain occur as the material is stressed. Accordingly, we use the Gibbs ensemble for calculations on nematic rubbers where phase transitions are observed. Mathematically it is easier to use the Helmholtz ensemble, which we do for the investigation of conventional, nonnematic, rubber where there are no discontinuous changes in the stress–strain response and we proceed with the analysis perturbatively.

4. Results

4.1. Results for Conventional, Nonnematic, Rubbers. One purpose of doing experiments on conventional rubbers is to enable subsequent predictions to be made of a rubber's properties under general deformation conditions. This information is encapsulated in the free energy density function, conventionally called W, which is a function of the invariants, I_i, of the Cauchy–Green deformation tensor.[28,29]

$$W = W(I_1,I_2)$$

$$I_1 = \lambda_x^2 + \lambda_y^2 + \lambda_z^2$$

$$I_2 = \frac{1}{\lambda_x^2} + \frac{1}{\lambda_y^2} + \frac{1}{\lambda_z^2} \tag{21}$$

where $I_3 = \lambda_x\lambda_y\lambda_z = 1$ because of the incompressibility of conventional rubbers. Since W is a free energy density, a general true stress can be written as

$$\sigma_i = \lambda_i\frac{\partial W}{\partial \lambda_i} = \lambda_i\left[\frac{\partial I_1}{\partial \lambda_i}\frac{\partial W}{\partial I_1} + \frac{\partial I_2}{\partial \lambda_i}\frac{\partial W}{\partial I_2}\right] \tag{22}$$

or

$$\sigma_z = 2\,(\lambda_z^2 - \lambda_y^2)(W_1 + \lambda_x^2 W_2)$$

$$\sigma_x = 2\,(\lambda_x^2 - \lambda_y^2)(W_1 + \lambda_z^2 W_2) \tag{23}$$

where $W_k = \partial W/\partial I_k$ for $k = 1$ and 2. In order to investigate W_1 and W_2 as fully as possible under general biaxial conditions, W_1 and W_2 are calculated either by varying I_1 at constant I_2 and vice versa[29] or by varying λ_x at constant λ_z.[30] An alternative which poses a demanding test of theory was suggested by Gottlieb and Gaylord.[14] One fits to some uniaxial data and then, using the fitting parameters obtained, compares with no further adjustment to a biaxial experiment. We therefore first fit to a Mooney plot and then compare with a pure shear experiment. Pure shear can be thought of as the combination of an extension in, say, the z direction, and a compression in a perpendicular direction, say y, to keep $\lambda_x = 1$. Alternatively, a tensile stress could be applied in the x direction to maintain $\lambda_x = 1$. Data for both of these experiments for a vulcanized isoprene rubber are available from the work of Kawabata et al.[30] For the uniaxial extension–compression experiment ($\lambda_x = \lambda_y = (\lambda_z)^{1/2}$) we obtain

$$\frac{\sigma_z}{\lambda_z^2 - 1/\lambda_z} = W_1 + \frac{1}{\lambda_z}W_2 \tag{24}$$

which is a constant in the Gaussian chain theory of elasticity where $W = W_1 I_1$.

For a pure shear experiment $I_1 = I_2$; therefore $\lambda_z = 1/\lambda_y$ and $\lambda_x = 1$, and we set two tensile stresses, σ_z to control λ_z and σ_x set to ensure $\lambda_x = 1$. A suitable quantity to plot vs λ_z is

$$\frac{\sigma_z}{\lambda_z^2 - 1/\lambda_z^2} = W_1 + W_2 \tag{25}$$

which measures deviations from classical elasticity for a pure shear experiment.[14]

$T \gg T_c$ corresponds to our interpretation of conventional rubbers as elastomers with nematic interactions but at temperatures far above the nematic–isotropic phase transition point. Accordingly, we expect any ordering induced by the stressing of the rubber to be small. In this regime we use perturbation theory to solve the diffusion equation to obtain $\lambda_{0,0}$ and the chain radii of gyration. In terms of the coupling constants, the answers are as follows to second order:

$$\lambda_{0,0} = \frac{(\Delta_Q^2)^2\tau}{4} + \frac{(\Delta_X^2)^2\tau}{3}$$

$$\frac{l_x}{l_0} = 1 - \frac{\Delta_Q^2}{6} + \frac{\Delta_X^2}{3} - \frac{4\Delta_Q^2\Delta_X^2}{45} + \frac{8(\Delta_X^2)^2}{135}$$

$$\frac{l_y}{l_0} = 1 - \frac{\Delta_Q^2}{6} - \frac{\Delta_X^2}{3} + \frac{4\Delta_Q^2\Delta_X^2}{45} + \frac{8(\Delta_X^2)^2}{135}$$

$$\frac{l_z}{l_0} = 1 + \frac{\Delta_Q^2}{3} + \frac{(\Delta_Q^2)^2}{15} - \frac{4(\Delta_X^2)^2}{135} \tag{26}$$

where $\tau = \bar{T}^2 - 2/15$ is a measure of the distance from the phase transition temperature. For example, if the chain is in a biaxial state with a large Q and a small finite X, eqs 26 show that the chain backbone adopts a transversely flattened prolate ellipsoidal shape with the long axis in the z direction.

Inserting these expressions into (18), we obtain the perturbation (Landau) free energy for the strained elastomer.

$$F_{\text{total}} = N_s(\mathcal{A}_1 + \mathcal{A}_2\Delta_Q^2 + \mathcal{A}_3\Delta_X^2 + \mathcal{A}_4\Delta_Q^2\Delta_X^2 + \mathcal{A}_5(\Delta_Q^2)^2 + \mathcal{A}_6(\Delta_X^2)^2 + \ldots) \tag{27}$$

where

$$\mathcal{A}_1 = \frac{1}{2}\left(\lambda_x^2 + \frac{1}{\lambda_x^2\lambda_z^2} + \lambda_x^2\right)$$

$$\mathcal{A}_2 = \frac{1}{12}\left(\lambda_x^2 + \frac{1}{\lambda_x^2\lambda_z^2} - 2\lambda_z^2\right)$$

$$\mathcal{A}_3 = \frac{1}{6}\left(\frac{1}{\lambda_x^2\lambda_z^2} - \lambda_x^2\right)$$

$$\mathcal{A}_4 = \frac{1}{90}\left(\frac{1}{\lambda_x^2\lambda_z^2} - \lambda_x^2\right)$$

$$\mathcal{A}_5 = \frac{1}{72}\left(\lambda_x^2 + \frac{1}{\lambda_x^2\lambda_z^2}\right) + \frac{\lambda_z^2}{45} + \frac{\tau}{4}\frac{L}{l_0} - \frac{1}{120}$$

$$\mathcal{A}_6 = \frac{7}{270}\left(\lambda_x^2 + \frac{1}{\lambda_x^2\lambda_z^2}\right) + \frac{2\lambda_z^2}{135} + \frac{\tau}{3}\frac{L}{l_0} - \frac{1}{90} \tag{28}$$

Differentiating (27) with respect to Δ_Q^2 and Δ_X^2 to minimize the free energy results in two simultaneous linear

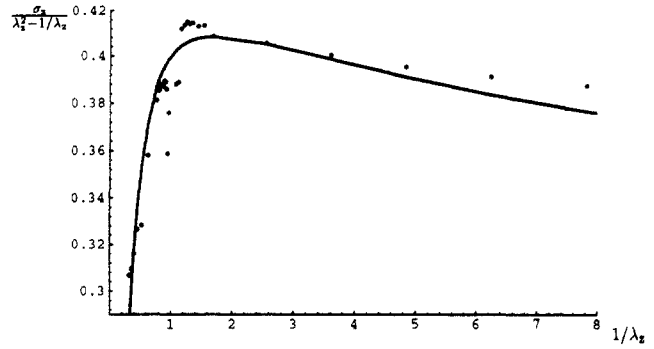

Figure 1. Mooney plot of an isoprene rubber using the data of Kawabata et al.[30] (black dots) together with the fit of the theory using $\tau L/l_0 = 1.8$ and $N_s k_B T = 0.437 \times 10^6$ J m^{-3}. These parameters were obtained using a least-squares method.

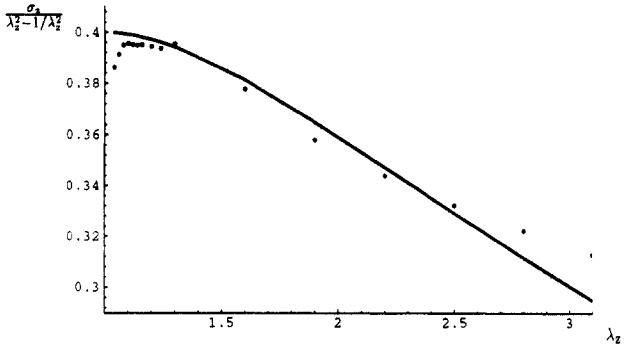

Figure 2. Plot of $\sigma_z/(\lambda_z^2 - 1/\lambda_z^2)$ vs λ_z for the same isoprene rubber sample as in Figure 1. The curve is the prediction of the theory using the fitting parameters determined by the fit in Figure 1.

equations for Δ_Q^2 and Δ_X^2. Solving these gives the equilibrium values $\Delta_Q^2(\tau L/L_0,\lambda_z,\lambda_x)$ and $\Delta_X^2(\tau L/l_0,\lambda_z,\lambda_x)$, which can then be substituted into eqs 19 to obtain the reduced stresses. Notice how to second order, the number of parameters reduces from three to two, since L/l_0 and τ only appear in the combination $\tau L/l_0$. The solutions are

$$\overline{\Delta_Q^2} = \frac{2\mathcal{A}_2\mathcal{A}_6 - \mathcal{A}_3\mathcal{A}_4}{\mathcal{A}_4^2 - 4\mathcal{A}_5\mathcal{A}_6}$$

$$\overline{\Delta_X^2} = \frac{2\mathcal{A}_3\mathcal{A}_5 - \mathcal{A}_2\mathcal{A}_4}{\mathcal{A}_4^2 - 4\mathcal{A}_5\mathcal{A}_6} \qquad (29)$$

For vanishing nematic influences the nematic interaction parameter $a \to 0$, the classical form of the uniaxial stress-optical law can be recovered. As $a \to 0$, $\bar{T}$ and hence $\tau \to \infty$. In this limit $\Delta_Q^2 \to -\mathcal{A}_2/2\mathcal{A}_5$. For uniaxial extension, $\lambda_z = \lambda$, $\lambda_x = \lambda_y = 1/(\lambda)^{1/2}$. Rewriting the expression for Δ_Q^2 in terms of Q and ignoring terms which are smaller than τ in $\mathcal{A}_5$, we obtain $Q = 1/(6L/l_0)(\lambda^2 - 1/\lambda) = 1/(6L/l_0)\sigma^*$, in agreement with ref 13.

Using these results, we first fit to a Mooney plot of data extracted from the work of Kawabata et al.[31] by a least-squares method. Figure 1 shows the resulting Mooney plot. The fit follows the data fairly closely except for close to $\lambda_z = 1$, where the spread in the experimental data gets worse (as two small quantities are being divided). The fitting parameters are $\tau L/l_0 = 1.8$ and $N_s k_B T = 0.437 \times 10^6$ J m^{-3}. The experiments were performed at $T = 293$ K, and one therefore obtains a strand density of 10^{26} per unit volume. Taking the density of isoprene, $-[-CH_2C(CH_3)=CHCH_2-]-$, as between 920 and 1000 kg m^{-3},[32] this equates to a chain length of 75–82 monomers. In ref 33, the chain length is quoted as 60 monomer units for a typical isoprene rubber, of the same order of magnitude as our estimate. The effective step length of isoprene in an unstrained state is between 4.7 and 5.5 monomer lengths.[32] Therefore there are 14–17 step lengths in a chain. This in turn allows the τ of the experiments to be estimated. The phase transition temperature of this system can then be estimated, to see if it indeed lies below or around the glass transition temperature of natural rubber. Since $\tau = \bar{T}^2 - 2/15$ we can deduce that a $\bar{T} = 293$ K corresponds to a $\bar{T}_{expt}$ between 0.486 and 0.514, whence $T_{NI} = (\bar{T}_{NI}/\bar{T}_{expt})T_{expt}$ lies between 220 and 233 K. (Recall $\bar{T}_{NI} = 0.38775$.) The glass transition temperature of natural rubber is ≈210 K, close to this estimate. The pure shear data from ref 30 is extracted and plotted according to (25) using the parameters obtained from the Mooney plot (Figure 1). As Gottlieb and Gaylord assert, prediction of biaxial behavior purely from uniaxially determined parameters is a stringent test of theory. The curve shown in Figure 2 follows the experimental points quite well for the first part of the data but does not show sufficient curvature in the latter half of the plot.

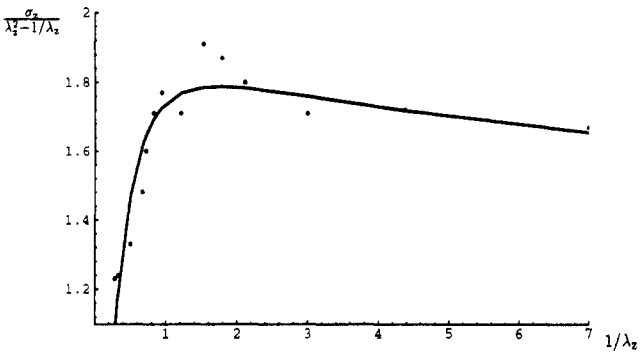

Figure 3. Mooney plot for the data of Rivlin and Saunders.[29] Our theory appears to fit these data considerably better than many competing (entanglement) theories of rubber elasticity.[34]

We also plot the classical data of Rivlin and Saunders for the uniaxial case. This is shown in Figure 3. The curve seems to be a better fit than many of the entanglement theories, which are compared by Gottlieb and Gaylord.[33] The Rivlin and Saunders data for pure shear do not approach the right zero shear modulus at low values of the stress, so we cannot compare our model with the pure shear results for those experimental data.

4.2. Results for Nematic Rubbers. First we present results for the case of uniaxial compression of a rubber. At the phase transition temperature, a monodomain of the rubber will undergo a spontaneous shape change from a spherical to a prolate ellipsoidal shape. Stressing a nematic rubber just above the uniaxial phase transition point has more interesting consequences. Pulling in the principal ordering direction induces a phase transition to a prolate uniaxial state. This case has been covered in earlier work.[13] If instead the rubber is compressed along the z axis, phase transitions to biaxial states occur. Figures 4–6 show the results of compressing in the z direction at different temperatures. The reduced temperatures shown have been divided by the reduced phase transition temperature of the melt $\bar{T}_c = 0.387\,75$. Figure 4 shows the order parameters Q and X vs the reduced stress σ_z^*, Figure 5 σ_z^* vs the extension ratios λ_x and λ_y, and Figure 6 $\sigma_z^*/(\lambda_z^2 - 1/\lambda_z)$ vs $1/\lambda_z$, all for a reduced chain length of $L/l_0 = 20$. As the rubber is compressed, it first forms a paranematic uniaxial oblate phase, with $X = 0$, $Q < 0$. As the stress is increased, there will be at some point a transition to a nematic state at some critical $\sigma_z^* = \sigma_c^*$. If

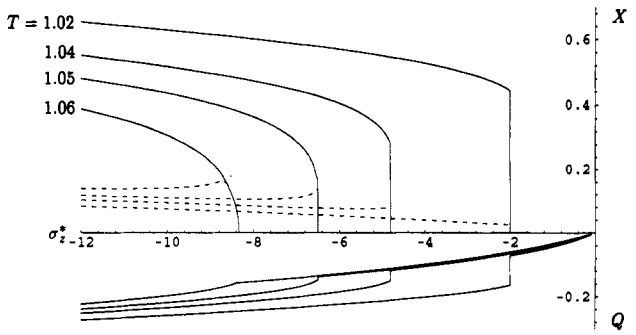

Figure 4. Order parameters Q and X vs σ^*_z for a nematic rubber in compression for four different reduced temperatures T, where T is measured in units of the melt transition temperature for the model, i.e., in units of $0.388(a\epsilon)^{1/2}/k_B$. The number of units in the chain is $L/l_0 \approx 20$. The dotted lines show the biaxiality extracted from the order parameter matrix as described in section 2. For T close to the melt transition temperature the transition is first order. Increasing T shifts the transition to higher σ_z^*. Beyond the critical temperature, $T \approx 1.055$, the transitions become second order. If the network is very close to the melt transition temperature, the biaxiality induced by the compressive stress is very small and the system is very nearly uniaxial; for example, when $T = 1.02$ then $X \approx -3Q$, the condition for the state to be uniaxial. After the transition, the order of the system continues to rise, as both X and Q increase monotonically. The real biaxiality decreases slightly and then slowly rises. After the transition, increasing the stress in the z direction increases order in the x direction.

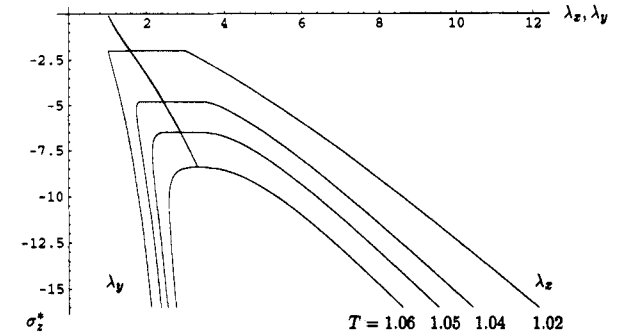

Figure 5. Stress σ_z^* plotted against the extension ratios λ_x and λ_y for the four different temperatures. Above the transition stress we have $\lambda_x = \lambda_y$; a monodomain of the rubber becomes an oblate spheroid. At the phase transition the rubber orders in the x direction and becomes like a prolate ellipsoid with the long axis in the x direction, squashed in the z direction. For the temperatures $T = 1.02$, 1.04, and 1.05, the phase transition is first order. At $T = 1.06$ and higher temperatures, the phase transition is second order.

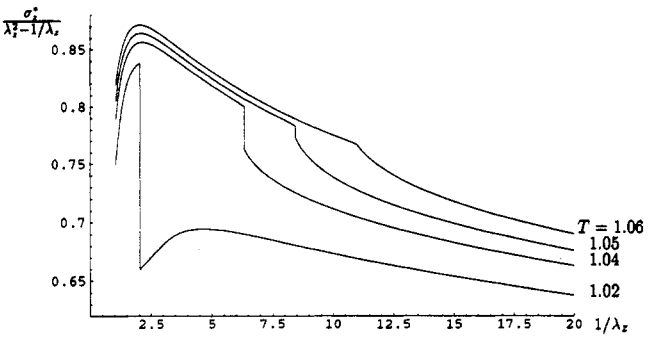

Figure 6. Reduced stress $\sigma_z^*/(\lambda_z^2 - 1/\lambda_z)$ vs $1/\lambda_z$ for the four different temperatures. The discontinuities for the three lower temperatures can be seen, as can the change in gradient for the second-order case when $T = 1.06$.

the rubber is close to the stress-free transition temperature, the transition to the nematic state will be first order, as is the case for $T = 1.02$, 1.04, and 1.05 in Figure 4. Q and X both show discontinuities at this point. Beyond a certain critical temperature the phase transition becomes second order, as is the case for $T = 1.06$ in Figure 4, where the apparent X rises smoothly from zero, and there is a change in the gradient of Q. At $T \approx 1.055$ there is therefore a tricritical point separating the first- and second-order regimes. The resulting nematic state is produced by the system choosing a direction in the xy plane in which to order. The choice of direction of ordering in the xy plane is arbitrary, and we choose to use the x direction. In practice, experimentally the ordering direction will presumably be chosen by any slight asymmetry in the applied stress. The nematic state produced is biaxial; i.e., the order parameter tensor (1) has three different numbers along the diagonal. The chains' chosen direction in the xy plane is the direction of the long axis of the prolate spheroid. Its z axis is shortened by the action of the compressive stress, thus creating a biaxial state. If the temperature is very close to the stress-free transition temperature, T_c, the stress required to drive the system into the nematic state is small and accordingly the amount of biaxiality in the nematic state is initially small, as the system is close to being a uniaxial state aligned in the x direction with little compression in the z direction. This is shown in Figure 4: recall that $X \approx -3Q$, the condition for describing a uniaxial state aligned in the x direction. The dotted lines in Figure 4 show the real biaxiality, extracted according to section 2, that is, the difference between the two smaller eigenvalues of the ordering tensor. It is apparent that as the phase transitions happen at larger magnitudes of σ_z^* the phase produced becomes more biaxial at formation, (cf. the sequence of increasingly negative transition stresses in Figure 4). Further increasing the magnitude of the stress beyond the transition point first results in a small fall in the real biaxiality, followed by a gradual rise. However, the system as a whole is becoming more ordered, as the values of Q and X increase monotonically; this must mean that the increase in ordering takes place in the prolate direction, so further compression in the z direction after the transition tends to elongate the rubber in the x direction. The phase transition becomes second order as the temperature is raised further above T_c as more stress has to be applied before the transition point is reached. This results in the polymer chains being forced further and further into the xy plane before the transition, and the system becoming more two-dimensional. A two-dimensional nematic phase transition is, for geometric reasons, second order. The stress–strain plots shown in Figures 5 and 6 have discontinuities at the transition stresses where the order parameters show discontinuities. In Figure 5, λ_x and λ_y bifurcate as the system becomes biaxial, in a continuous way if the transition is second order and discontinuously if the transition is first order. In Figure 6 the stress has been reduced by $\lambda_z^2 - 1/\lambda_z$ and plotted vs $1/\lambda_z$ to separate the curves from one another, so that the discontinuities could be better observed.

In order to investigate the system under a general biaxial stress, we have to choose what biaxial conditions to impose. In nematic rubbers we do not have the opportunity of doing the same kinds of experiments that are possible on conventional rubbers, such as maintaining I_1 constant and varying I_2, due to the phase transitions. Therefore we choose two quite arbitrary ways to look at the effect of biaxial stress on nematic rubbers: (i) We investigate the effect of a small constant extensional stress acting in the x direction while compressing in the z direction, to see how this second stress affects the behavior of the system. (ii) We fix as constant the ratio between two applied

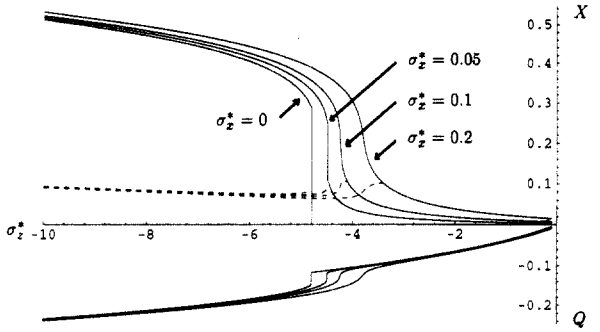

Figure 7. Order parameters Q and X for $T = 1.04$ and $L/l_0 = 20$ vs σ_z^* with small constant tensile stresses σ_x^* applied in the x direction. The dotted lines show the real biaxiality as described in section 2. Initially, when σ_z^* is small, the system forms a biaxial paranematic phase. If the transverse stress σ_x^* is small enough, i.e., less than ≈0.05, there will be a phase transition to a biaxial nematic state. The phase transition critical stress is reduced in magnitude by the application of the small stress. If σ_z^* is too large, there is no phase transition and the order in both Q and X increases smoothly from their values at $\sigma_z^* = 0$.

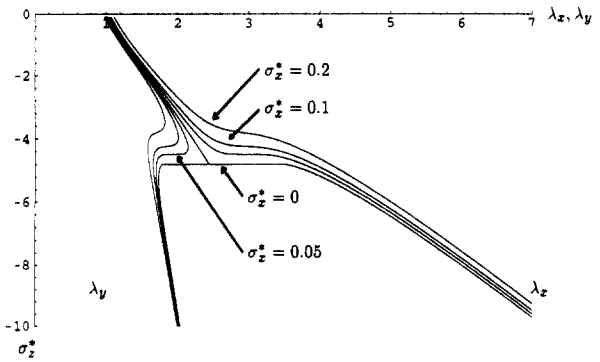

Figure 8. σ_z^* vs λ_x and λ_y for $T = 1.04$ and $L/l_0 = 20$ at various values of constant transverse tensile stress σ_x^*. For σ_x^* greater than ≈0.05, there is no phase transition.

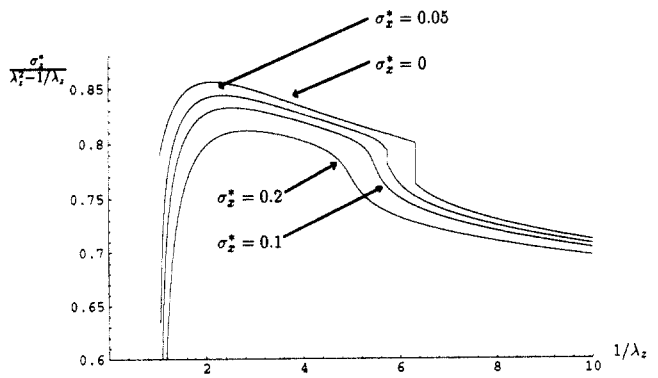

Figure 9. $\sigma_z^*/(\lambda_z^2 - 1/\lambda_z)$ vs $1/\lambda_z$ for $T = 1.04$ and $L/l_0 = 20$ at the indicated values of σ_x^*.

stresses $\sigma_z^* = 2\sigma_x^*$ and investigate the resulting stress–strain response.

In Figures 7–9 the effects of applying a small constant extensional stress σ_x^* while compressing in the z direction, are shown for the temperature $T = 1.04$ with $L/l_0 = 20$. Figure 7 shows the order parameters Q and X vs σ_z^* at values of σ_x^* of 0, 0.05, 0.1, and 0.2. Figure 8 shows σ_z^* vs λ_x, λ_y, and Figure 9 shows $\sigma_z^*/(\lambda_z^2 - 1/\lambda_z)$ vs $1/\lambda_z$, all for the same set of values of σ_x^*. The small stress σ_x^* lowers the stress σ_z^* needed in the z direction to cause a phase transition. Above a certain value of the stress σ_x^* there is no phase transition, so the line of phase transitions ends with a critical point. The biaxial stress first induces a biaxial paranematic state with $Q \neq 0, X \neq 0$. Below $\sigma_x^* = 0.05$, increasing σ_z^* causes a first-order phase transition to a biaxial state, so the values of Q and X show

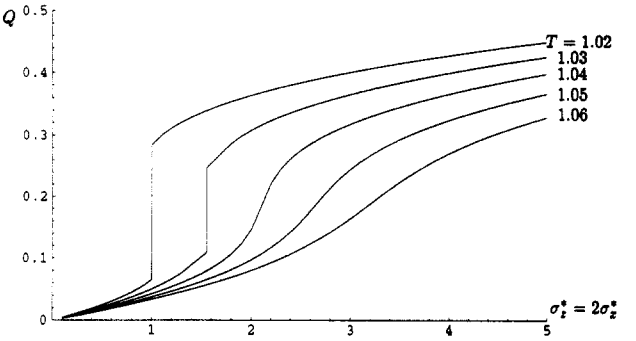

Figure 10. Order parameter Q vs σ_z^* for the case where a constant ratio $\sigma_z^* = 2\sigma_x^*$ is maintained. The number of step lengths in the chains is $L/l_0 = 20$. When σ_z^* is small, a paranematic biaxial phase is formed. If T is sufficiently small, then there is a first-order phase transition to a biaxial nematic phase, as when $T = 1.02$ and 1.03. If the temperature is higher, there is no phase transition, just a smooth transition from a less ordered to a more ordered state.

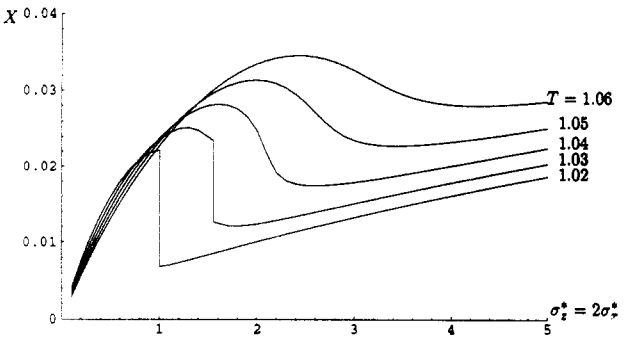

Figure 11. Order parameter X vs σ_z^* for the case where a constant ratio of $\sigma_z^* = 2\sigma_x^*$ is maintained. Since Q is positive, X in this case measures the real biaxiality of the system, i.e., the difference in the two small elements of the order parameter. Initially when σ_z^* is small the system forms a paranematic biaxial phase. If the temperature is low enough, as is the case for $T = 1.02$ and 1.03, then there is a first-order phase transition to a biaxial nematic phase. Since σ_z^* is larger than σ_x^*, the system forms a prolate ellipsoidal phase aligned along the z direction, slightly elongated in the x direction. The increase in ordering in the z direction destroys the ordering in the x direction, resulting in a fall in X as the system becomes more ordered. Above $T \approx 1.03$, the resulting fall in X becomes a smooth change and would presumably be eliminated at much higher temperatures.

discontinuities at these points, as do the extension ratios. When there is no phase transition, the order parameters and strains vary continuously. The dotted lines in Figure 7 show the real biaxiality. X measures the real biaxiality until the phase becomes more ordered and prolate ellipsoidal along the x direction, whereupon the real biaxiality then increases slowly with increasing stress. The diagram of the order parameters, Figure 7, is reminiscent of a nematic ordering in an external field. In this case the analogy would have to be of the ordering of a genuinely biaxial nematic, with σ_z^* acting as the temperature and σ_x^* as the applied field.

Figures 10–13 show the results for stressing with a constant ratio $\sigma_z^* = 2\sigma_x^*$. Figures 10 and 11 show Q and X vs σ_z^*, respectively, with $L/l_0 = 20$. Stressing again results in a biaxial paranematic phase, and if T is small enough, further stress results in a phase transition to a nematic state, as is the case for $T = 1.02$ and 1.03. Since $\sigma_z^* > \sigma_x^*$, the nematic state will have its long axis aligned along the z direction. The process of creating strong alignment in the z direction reduces the amount of ordering possible in the xy plane as implied by eq 4. X therefore falls as Q increases. If the ordering takes place via a first-order phase transition, the falls in X and the rise in Q will

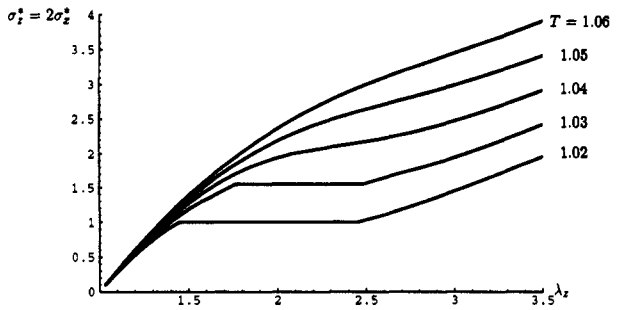

Figure 12. Stress σ_z^* vs λ_z for the case where a constant ratio of $\sigma_z^* = 2\sigma_x^*$ is maintained. At small values of σ_z^* the system forms a biaxial paranematic phase. For $T = 1.02$ and 1.03, there is a first-order phase transition to a biaxial nematic phase. At higher temperatures there is no phase transition.

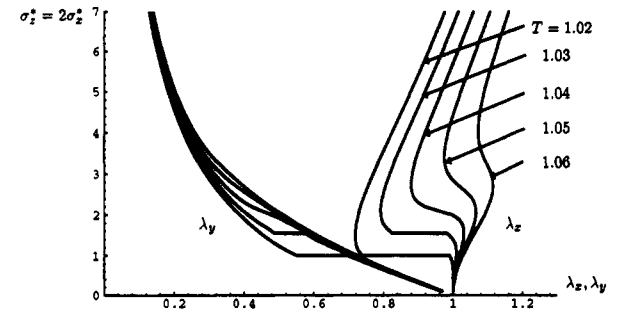

Figure 13. Stress σ_z^* vs λ_x and λ_y for the case where a constant ratio of $\sigma_z^* = 2\sigma_x^*$ is maintained. The number of step lengths in the chains is $L/l_0 = 20$. As the stress rises from zero, a biaxial paranematic phase is formed, λ_x increasing and λ_y decreasing. As the stress rises, the system starts to order strongly in the z direction, the direction of greatest stress; λ_z and λ_y start to decrease. The increasing order in the z direction, measured by Q, directly reduces the order in the perpendicular direction, measured by X. (See eq 4 in the text.) This causes a reduction in the perpendicular size of the sample. If the temperature is low enough, $T = 1.02$ and $T = 1.03$, there is a first-order transition to a biaxial nematic state. The first order rise in Q and reduction in X causes the discontinuous reduction in λ_x and λ_y. If there is no phase transition, as for the case of $T = 1.04$ and higher, then the changes in λ_x and λ_y are smooth but follow the same pattern as before.

be discontinuous, as will the effect on the strains. Figure 12 shows σ_z^* vs λ_z, showing the discontinuous change in λ_z at $T = 1.02$ and 1.03. Figure 13 shows σ_z^* vs λ_x and λ_y. λ_x increases initially; λ_y decreases. At the phase transition both fall discontinuously due to the jump in λ_z. If there is no phase transition, as happens at higher temperatures ($T = 1.04$ and $T = 1.05$), λ_x, λ_y, and λ_z show the same sort of behavior but with continuous changes in their values.

5. Conclusions

In this paper we have developed a theory of nematic rubber that can be subjected to general biaxial deformations. The theory accounts for nematic interactions using a mean field where all interacting particles have cylindrical symmetry. The model predicts that biaxial phases occur under both uniaxial and biaxial stresses and that both first- and second-order phase transitions are possible, depending upon the prevailing temperature and stress. The deviations away from classical rubber behavior of such a rubber well above the phase transition temperature were found to agree well with experiment, better in some cases than competing entanglement theories of rubber. We therefore conclude that nematic effects can play an important part in determining the physical characteristics of a conventional rubber.

References and Notes

(1) De Gennes, P. G. *C.R. Acad. Sci. Ser.* **1975**, *B281*, 101.
(2) De Gennes, P. G. In *Polymer Liquid Crystals*; Ciferri, A., Krigbaum, W. R., Meyer, R. B., Eds.; Academic: New York, 1982; p 115.
(3) Legge, C. H.; Mitchell, G. R.; Davis, F. J. 1990 Annual Conference of British Liquid Crystal Society, Bristol, 9–11th April, 1990; p 16.
(4) Davis, F. J.; Gilbert, A.; Mann, J.; Mitchell, G. R. *J. Polym. Sci., Part A: Polym. Chem.* **1990**, *28*, 1455.
(5) Legge, C. H.; Davis, F. J.; Mitchell, G. R. *J. Phys. 2* **1991**, *10*, 1253.
(6) Schätzle, J.; Kaufhold, W.; Finkelmann, H. *Makromol. Chem.* **1989**, *190*, 3269.
(7) Kupfer, J.; Finkelmann, H. *Macromol. Chem., Rapid Commun.* **1991**, *12*, 717.
(8) Kaufhold, W.; Finkelmann, H.; Brand, H. R. *Macromol. Chem.* **1991**, *192*, 2555.
(9) Warner, M.; Gelling, K. P.; Vilgis, T. A. *J. Chem. Phys.* **1988**, *88*, 4008.
(10) Deloche, B.; Samulski, E. T. *Macromolecules* **1988**, *21*, 3107.
(11) Abramchuk, S. S.; Khokhlov, A. R. *Dokl. Akad. Nauk. SSSR* **1987**, *297*, 385; *Dokl. Phys. Chem. (Engl. Transl.)* **1988**.
(12) Jarry, J. P.; Monnerie, M. *Macromolecules* **1979**, *12*, 316.
(13) Warner, M.; Wang, X. J. *Macromolecules* **1991**, *24*, 4932.
(14) Gottlieb, M.; Gaylord, R. J. *Macromolecules* **1987**, *20*, 130.
(15) DiMarzio, E. A. *J. Chem. Phys.* **1962**, *36*, 1563.
(16) Jackson, J. L.; Shen, M. C.; McQuarrie, D. A. *J. Chem. Phys.* **1966**, *44*, 2388.
(17) Tanaka, T.; Allen, G. *Macromolecules* **1977**, *10*, 426.
(18) Gao, J. *Macromolecules* **1991**, *24*, 5179.
(19) Gramsbergen, E. G.; Longa, L.; de Jeu, W. H. *Phys. Rep.* **1986**, *135* (4), 195.
(20) Zannoni, C. In *The Molecular Physics of Liquid Crystals*; Luckhurst, G. R.; Gray, G. W., Eds.; Academic Press: London, 1979.
(21) Jähnig, F. *J. Chem. Phys.* **1979**, *70*, 3279.
(22) Warner, M.; Gunn, J. M.; Baumgärtner, A. *J. Phys. A: Meth. Gen.* **1985**, *18*, 3007.
(23) Ten Bosch, A.; Maissa, P.; Sixou, P. *Phys. Lett.* **1983**, *94A*, 299; *J. Chem. Phys.* **1983**, *79*, 3462.
(24) Rusakov, V. V.; Shliomis, M. I. *J. Phys. Lett.* **1986**, *46*, L-935.
(25) Saitô, N.; Takahashi, K.; Yunoki, Y. *J. Phys. Soc. Jpn.* **1967**, *22*, 219.
(26) Meixner, J.; Schäfke, F. M. *Mathieusche Funktionen und Sphäroidfunctionen*; Springer: Berlin, 1954.
(27) Renz, W.; Warner, M. *Proc. R. Soc. London* **1988**, *A417*, 213.
(28) Wang, X. J.; Warner, M. *J. Phys. A: Math. Gen.* **1986**, *19*, 2215.
(29) Mooney, M. *J. Appl. Phys.* **1940**, *11*, 582. Rivlin, R. S. *Philos. Trans. R. Soc. London, A* **1948**, *A241*, 379.
(30) Rivlin, R. S.; Saunders, D. W. *Philos. Trans. R. Soc. London, A* **1951**, *A243*, 251.
(31) Kawabata, S.; Matsuda, M.; Tei, K.; Kawai, H. *Macromolecules* **1981**, *14*, 154.
(32) Brandrup, J.; Immergut, E. H.; Eds. *Polymer Handbook*, 3rd ed.; Wiley-Interscience: New York, 1989.
(33) Roe, R. J.; Krigbaum, W. R. *J. Polym. Sci.* **1962**, *61*, 167.
(34) Gottlieb, M.; Gaylord, R. J. *Polymer* **1983**, *24*, 1644.